

Are your **MRI contrast agents** cost-effective?

Learn more about generic **Gadolinium-Based Contrast Agents**.



**FRESENIUS  
KABI**

caring for life

**AJNR**

**Computerized Assessment of Angiographic  
Occlusion Rate and Coil Density in  
Embolized Human Cerebral Aneurysms**

C. Sherif, G. Bavinski, C. Dorfer, F. Kanz, E. Schuster and  
H. Plenk, Jr

This information is current as  
of April 17, 2024.

*AJNR Am J Neuroradiol* 2009, 30 (5) 1046-1053

doi: <https://doi.org/10.3174/ajnr.A1463>

<http://www.ajnr.org/content/30/5/1046>

**ORIGINAL  
RESEARCH**

C. Sherif  
G. Bavinzski  
C. Dorfer  
F. Kanz  
E. Schuster  
H. Plenk, Jr

# Computerized Assessment of Angiographic Occlusion Rate and Coil Density in Embolized Human Cerebral Aneurysms

**BACKGROUND AND PURPOSE:** Computerized methods have been introduced for more objective quantification of angiographic occlusion rate and coil density as parameters of successful embolization. This study aimed 1) to evaluate this new computerized method for angiographic occlusion rating and coil density calculations by comparison with corresponding histometric parameters from retrieved human aneurysms, and 2) to compare the new computerized method with the present standard of subjective angiographic occlusion rating.

**MATERIALS AND METHODS:** From 14 postmortem-retrieved human aneurysms, angiographic occlusion rate was determined by contrast medium attenuation-gradient distinction on digital subtraction angiographs after Guglielmi detachable coil (GDC) embolization. Angiographic coil density was calculated, approximating aneurysms as ellipsoid and coils as cylindrical volumes. On surface-stained histologic ground sections of the respective aneurysms, the occluded aneurysm area and coil area were measured. Then, we calculated and compared the histometric occlusion rates and coil densities with the corresponding angiographic parameters by using the Wilcoxon paired signed-rank test and the Spearman rank correlation.

**RESULTS:** Computerized angiographic occlusion rates (75%–100%) showed good correlation ( $r = 0.799$ ;  $P < .01$ ) with histometric occlusion-rates (61%–100%), resulting in no statistically significant differences ( $P = .2163$ ). With 5.1% ( $\pm 3.8$ ), the mean difference between computerized angiographic occlusion rates and histometry was substantially lower compared with 10.7% ( $\pm 8.7$ ) mean difference between subjective angiographic estimations and histometry. Calculated angiographic coil density (13%–32%) significantly differed from histometric coil density (8%–35%;  $P < .05$ ).

**CONCLUSIONS:** For recanalized aneurysms, computerized angiographic occlusion rating showed better correspondence with histometry compared with subjective angiographic occlusion rating. Clinical application of this new tool may lead to more objective cutoff values for re-embolization indications. The value of coil density calculations seems limited by the approximation of the aneurysms as ellipsoid volumes.

Endovascular embolization is a widely accepted alternative treatment to surgical clipping in the therapy of cerebral aneurysms.<sup>1–3</sup> Besides many clinical studies proving the efficacy of this therapeutic option,<sup>4–6</sup> only a few human case studies have analyzed thrombus formation and organization, tissue reactions to coil implants, orifice endothelialization, and aneurysm recanalization in the course of time,<sup>7–13</sup> none of them providing histometric quantification.

Recently, a morphometric quantification of angiographic and histologic images from experimental aneurysms showed that computerized evaluation of postembolization angiographic occlusion rates would be more accurate compared with subjective angiographic occlusion rate estimations.<sup>14</sup> For the first time, this new method of quantification allowed an objective comparison of the results of independent experimental studies.<sup>15</sup> Therefore, the next consequent step was to test these methods of quantification on angiographic and histologic images of retrieved human aneurysms. With a proof of sufficient correlation also in human aneurysms, this comput-

erized method could be clinically introduced to augment, or even replace, the rather rough subjective estimations of angiographic occlusion rating presently in use.

Furthermore, calculation of angiographic coil density was envisaged recently in several volumetric studies.<sup>16–20</sup> A comparison with histometrically assessed coil density in real aneurysm morphology would show if this angiographic parameter could be implemented into clinical routine.

In our study, these new computerized methods for the quantification of angiographic and histomorphologic occlusion rates and coil densities were applied to a series of retrieved embolized human cerebral aneurysms.

The study aims consisted of the following:

1. To assess for the correlation of computerized angiographic occlusion rating and coil density calculations compared with the respective histometric parameters of corresponding histologic ground sections that display the intra-aneurysmal morphologic features with the highest available resolution power.
2. To compare computerized angiographic occlusion rating with the present clinical standard of subjective angiographic occlusion rate estimations. This comparison is performed by comparing both angiographic techniques with the corresponding histometric occlusion rates to assess for possible clinically relevant benefits of computerized angiographic occlusion rating.

Received June 13, 2008; accepted after revision November 19.

From the Department of Neurosurgery (C.S., G.B., C.D.), Department of Bone and Biomaterials Research at the Institute for Histology and Embryology (F.K., H.P. Jr), and Core Unit on Medical Statistics (E.S.), Medical University Vienna, Vienna, Austria.

Please address correspondence to Camillo Sherif, MD, Department of Neurosurgery, Medical University Vienna, Waehringer Guertel 18-20, A-1090 Vienna, Austria; e-mail: camillo.sherif@meduniwien.ac.at

DOI 10.3174/ajnr.A1463

**Patient characteristics, angiographic and histometric data**

Patient Data					Angiographic Data					Histometric Data			
No.	Loc	Sex/ Age F, M/y	Initial H&H	Survival, Days	Subj OR %	Neck width, mm	Length, mm	Comp OR%	Calc CD %	Neck width, mm	Length, mm	Histom OR %	Histom CD %
<b>1</b>	<b>AcomA</b>	<b>M/35</b>	<b>4</b>	<b>2</b>	<b>100</b>	<b>3.21</b>	<b>6.07</b>	<b>96</b>	<b>27</b>	<b>2.80</b>	<b>5.61</b>	<b>98</b>	<b>21</b>
2	PcomA	F/43	5	3	95	3.20	8.72	88	22	3.10	6.75	76	17
3	PcomA	F/43	5	3	100	3.22	5.48	94	24	3.13	6.07	97	35
<b>4</b>	<b>AcomA</b>	<b>F/70</b>	<b>4</b>	<b>4</b>	<b>95</b>	<b>2.87</b>	<b>6.83</b>	<b>74</b>	<b>13</b>	<b>2.46</b>	<b>7.32</b>	<b>61</b>	<b>8</b>
5	PICA	M/32	3	11	100	3.81	7.58	<b>92</b>	32	3.71	6.84	88	26
<b>6</b>	<b>AchoA</b>	<b>F/44</b>	<b>4</b>	<b>12</b>	<b>95</b>	<b>6.68</b>	<b>9.18</b>	<b>84</b>	<b>29</b>	<b>5.37</b>	<b>8.81</b>	<b>89</b>	<b>27</b>
7	PcomA	F/28	4	12	95	2.82	4.54	95	14	2.79	5.50	96	12
<b>8</b>	<b>Bas bif</b>	<b>M/52</b>	<b>4</b>	<b>12</b>	<b>100</b>	<b>5.01</b>	<b>8.69</b>	<b>93</b>	<b>16</b>	<b>4.11</b>	<b>6.73</b>	<b>87</b>	<b>17</b>
9	Bas bif	F/49	3	15	95	3.98	6.83	82	23	4.12	6.50	91	22
10	Bas bif	F/41	2	17	f/47	4	18	100	32	6.20	8.98	93	21
11	PcomA					5.43	11.62	93	24	4.81	11.93	85	18
12	OphtA	F/31	4	22	95	4.71	8.16	84	23	3.85	8.62	82	12
<b>13</b>	<b>Bas bif</b>	<b>F/43</b>	<b>4</b>	<b>36</b>	<b>95</b>	<b>6.05</b>	<b>12.06</b>	<b>89</b>	<b>26</b>	<b>4.81</b>	<b>11.26</b>	<b>85</b>	<b>15</b>
14	Bas bif	F/40	3	41	100	5.71	11.34	100	29	4.51	10.12	100	26

**Note:**—AchoA, anterior choroidal artery; AcomA, anterior communicating artery; Bas bif, basilar bifurcation; Calc CD, calculated coil density; Comp OR, computerized occlusion rate; F, female; H&H, Hunt and Hess grade; Histom CD, histometric coil density; Histom OR, histometric data and histometric occlusion rate; Loc, location; M, male; OphtA, ophthalmic artery; PcomA, posterior communicating artery; PICA, posterior inferior cerebellar artery; Subj OR, subjective occlusion rate;

**Materials and Methods**

**Aneurysm Selection**

For our study, 9 aneurysms were selected from 17 retrieved embolized human aneurysms from a previous study.<sup>13</sup> There were 8 aneurysms that had to be excluded because of insufficient correspondence of the ground section with the available digital subtraction angiography (DSA) projections (4 aneurysms) or because of shrinking artifacts of the ground sections mainly caused by insufficient perfusion-fixation (4 aneurysms). However, another 5 newly retrieved aneurysms meeting the selection criteria could be included (see aneurysms in bold letters in the accompanying Table). All 14 aneurysms had ruptured and were embolized with use of the Guglielmi detachable coil (GDC) system (Target Therapeutics/Boston Scientific, Fremont, Calif) according to manufacturer instructions.

**Subjective Estimation of Angiographic Occlusion Rate**

After each embolization procedure, the occlusion rate of each aneurysm was subjectively estimated on DSA according to Roy et al<sup>21</sup> by an experienced endovascular neurosurgeon: total occlusion (Roy class 1) was then defined as 100% occlusion rate, residual neck filling (Roy class 2) as 95% occlusion rate, and residual aneurysm filling (Roy class 3) as a less than 90% occlusion rate.

**Quantitative Computerized Angiographic Evaluations**

On calibrated images of the respective DSAs, 1 to 2 projections were selected for evaluation. The selection criterion was to obtain a representative overview of the aneurysm occlusion focusing on the recanalized neck, together with the length axis of the aneurysms. In a total of 6 cases with more complex aneurysmal anatomy, a second DSA projection was evaluated to minimize measurement inaccuracy. After digitalization and standardized image processing, the following angiographic parameters were defined by Adobe Photoshop 7.0 (Adobe Systems, San Jose, Calif). The selection of the DSA projections and the following definitions of the angiographic parameters were performed by the same experienced endovascular neurosurgeon who had subjectively estimated the angiographic occlusion rate. Computerized measurements were then performed by another physician blinded to the previous evaluations. We made all quantitative measurements of

the following defined angiographic parameters (in mm, or in mm<sup>2</sup>) by using the image analysis software “Lucia G” (LUCIA, Prague, Czech Republic).

**Total aneurysm area (mm<sup>2</sup>).** Borders of the contrast medium or coil-filled aneurysm and the orifice plane were outlined (Fig 1C). If the outline of the aneurysm could not be defined precisely on the DSA image(s) alone, the contours of the corresponding pretreatment angiogram were superimposed over the postembolization DSA image.

**Aneurysm neck width (mm).** Distance of the orifice plane, where the cranial borders of the parent arteries merged with the aneurysm outline (Fig 1C).

**Aneurysm maximal length (mm).** The longest distance between the orifice plane and the visible fundus of the aneurysm.

**Aneurysm maximal width (mm).** The longest distance between the 2 borders of the aneurysm outline parallel to the orifice plane. This parameter of “aneurysm height” was necessary for the calculation of the aneurysm ellipsoid volume.

**Aneurysm nonoccluded area (mm<sup>2</sup>).** The area filled or refilled by contrast medium within the total aneurysmal area was defined on the posttreatment DSA with use of an attenuation-gradient-based distinction. The attenuation range of gray levels of the radiopaque contrast medium in the aneurysm was defined by the attenuation range of the contrast medium in the parent arteries. On the basis of this range within the 256 gray levels of the digital image, the contrast medium-filled area was distinguished and false-color labeled for measurement (Fig 1C).

In the cases of 2 evaluated DSA projections, the mean values of the respective parameters were calculated.

**Calculation of Computerized Angiographic Occlusion Rate**

Finally, the occluded area of the aneurysm was calculated as the difference of “total area” minus “nonoccluded area” and was given as computerized angiographic occlusion rate (OR) in percentage.

**Calculation of Angiographic Coil Density**

We calculated the theoretic aneurysm and coil volume according to Tamatani et al<sup>16</sup> and Yoshino et al,<sup>17</sup> by using an equation approxi-

INTERVENTIONAL ORIGINAL RESEARCH

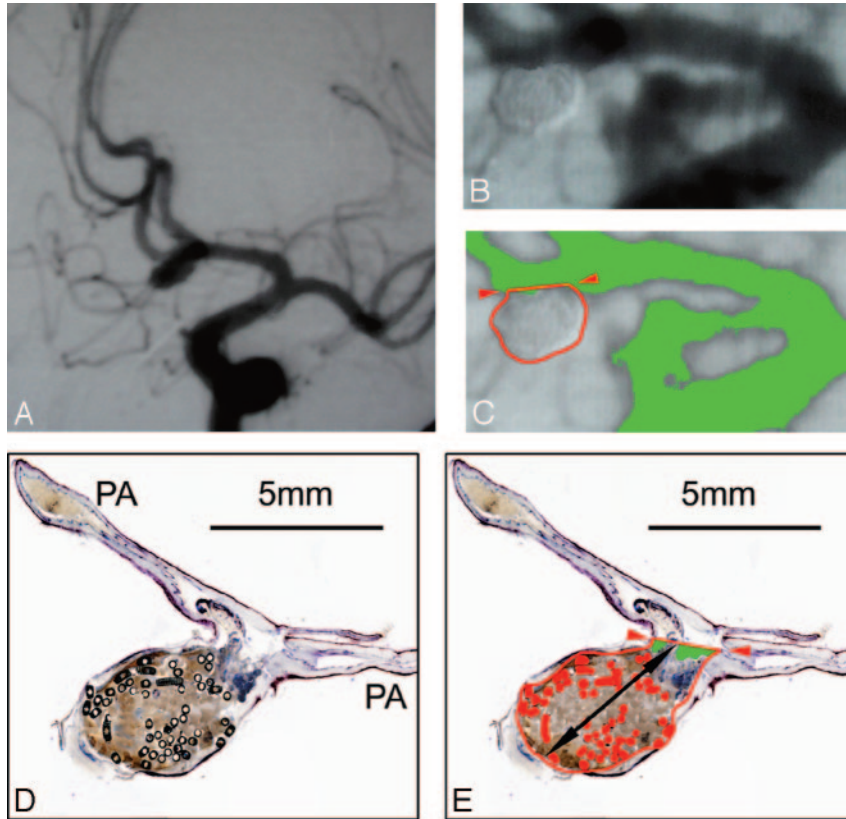


**Fig 1.** A–C, Anterior communicating artery aneurysm #1 (male patient; age, 35 years; survival, 2 days) with subjective occlusion rating of 100% and computerized occlusion rating of 96%. A, Preinterventional angiograph. B and C, Enlarged details of the postembolization DSA. C, Aneurysmal border is outlined in red, the neck plane with red arrows. The green false-color labeling of the contrast medium shows minimal inflow in the neck region. D and E, Micrographs (barr 5 mm) of 1 surface-stained ground section of aneurysm #1 through the neck region and the parent arteries. In 1E, the aneurysmal sac is outlined in red, the orifice plane with red arrows, and the total length in black. The metallic coil sections are false-color labeled in red, and the recanalized areas (D) are green labeled. In the center of the aneurysm, fresh red static thrombus, the basis for subsequent granulation tissue organization, can be seen.

mating an ellipsoid-shaped volume of the aneurysm: Aneurysm Volume =  $(4/3) \times \Pi \times (\text{total length}/2) \times (\text{height}/2)^2$ .

We calculated the coil volume of each inserted coil by using the equation of a cylindrical volume assuming the cylindrical shape of the GDC: Coil Volume =  $\Pi \times (\text{outer diameter}/2)^2 \times \text{length}$ . The outer diameter of each GDC is published by Target Therapeutics (Boston Scientific). Calculated angiographic coil density (%) was defined as the sum of all inserted coil volumes within the aneurysmal volume and calculated as volume fraction or percentage.

### Specimen Preparation and Histometric Evaluations

The techniques for the ground section preparation of the retrieved human aneurysms with the coils in situ and the procedures of digital photo documentation, image processing, and calibration with Adobe Photoshop 7.0 are described elsewhere.<sup>13–15,22</sup> Ground-section planes were selected to show a representative overview of the aneurysmal occlusion focusing on the neck plane, together with the length axis of the aneurysm in accordance with the respective DSA projections. For every aneurysm, histomorphologic structures were outlined on digitized calibrated images from 2 to 4 surface-stained (Sanderson Rapid Bone Stain solution (SURGIPATH Medical, Richmond, Va) ground sections. Then, in a second step, a physician blinded to the previous measurements measured direct histometric parameters (in mm, or in  $\text{mm}^2$ ) by using the image analysis software Lucia G:

**Total aneurysm area ( $\text{mm}^2$ ).** Defined by the internal boundary of the aneurysm wall and the orifice plane of the aneurysm between the neck points (Fig 1E).

**Aneurysm neck width (mm).** The distance of the orifice plane between the 2 neck points, where the walls of the parent arteries ended (marked by interruption of the inner elastic membrane) and merged into the aneurysmal walls (Fig 1E).

**Aneurysm maximal length (mm).** The longest distance between the orifice plane and the visible fundus of the aneurysm (Fig 1E).

**Nonoccluded area ( $\text{mm}^2$ ).** All inflow spaces not filled by fresh red or organized thrombi, and/or by coils in the total area of the aneurysm (Fig 1E).

**Coils area ( $\text{mm}^2$ ).** To define the area occupied by metallic coils, again an attenuation-gradient–based distinction of all nontransparent (= metallic) GDC sections in the surface-stained ground section was used. All distinguished coil areas were false-color labeled, lumina within coils were interactively filled, and the coil area was then defined as the sum of all coil areas within the total area of the aneurysm (Fig 1E). The mean values of the evaluated 2 to 4 ground sections were calculated for each parameter.

Finally, the following indirect histometric parameters were calculated:

- Histometric occluded area ( $\text{mm}^2$ ) as “total area” minus “nonoccluded area”
- Histometric occlusion rate (OR) in percentage as the relative proportion of the “occluded area” in percent of “total area”
- Histometric coil density (%) as the relative proportion of the “coil area” in percentage of “total area”

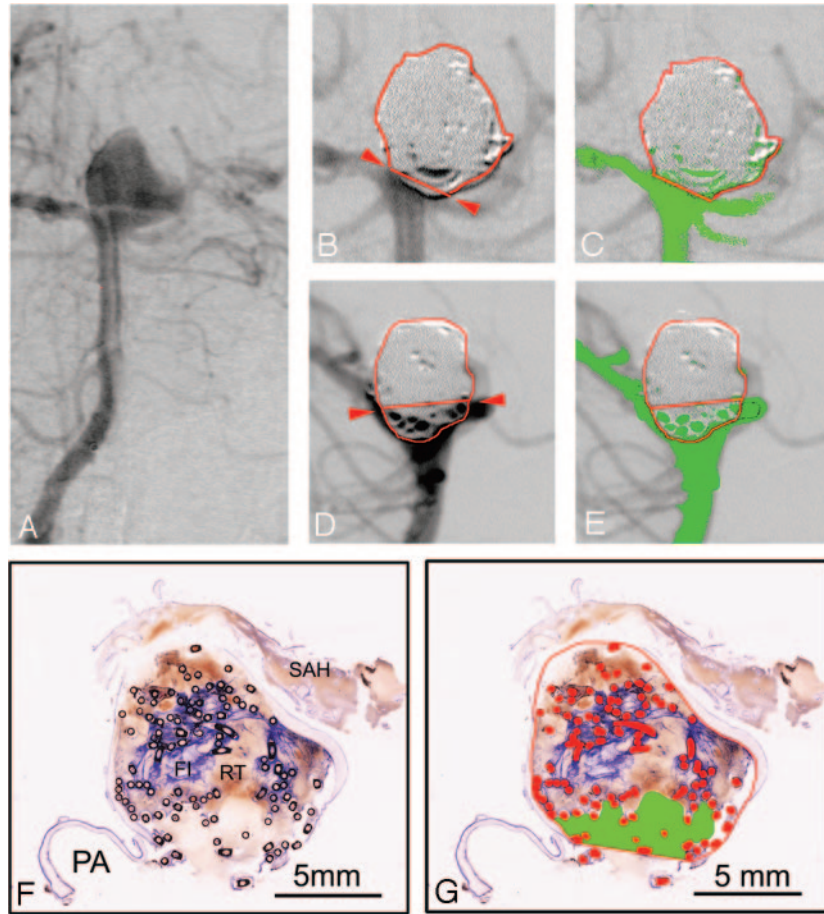


**Fig 2.** A–E, Basilar bifurcation aneurysm #13 (female patient; age, 43 years; survival, 36 days) with a subjective occlusion rate of 95% and a computerized occlusion rate of 89%. A, Preinterventional anteroposterior angiograph. B and C, Enlarged details of the postembolization anteroposterior DSA, the aneurysmal border in red and neck plane outlined with red arrows. C, Residual filling (green areas) in the aneurysmal neck region. D and E, Enlarged details of the postembolization lateral DSA projection, showing a larger contrast medium inflow area (green in 2E) between coil loops protruding caudally over the neck plane. F and G, Micrographs (bar 5 mm) of 1 surface-stained ground section of aneurysm #13 through the neck region and 1 parent artery (PA). F, Note the attenuated blue-stained fibrin clot (FI) and red thrombus (RT) in the center, and the subarachnoid hemorrhage (SAH). G, Aneurysmal border, orifice plane, and metallic coil sections are outlined and labeled in red. Some coil loops are protruding the orifice plane, and the inflow area, appearing pale stained without red thrombus in 2F, is labeled in green.

### Comparison of Angiographic and Histometric Parameters

We compared computerized angiographic occlusion-rating and coil-density calculations with the respective histometric parameters by using the nonparametric 2-tailed Wilcoxon paired signed-rank test. A *P* value of less than .05 was considered statistically significant. In cases of nonsignificant results, we performed a power analysis by using an assumed difference of 10% for  $\beta = 0.9\%$  and 5% for  $\beta = 0.7$ , respectively. To assess for agreement between the parameters, we supplemented the Wilcoxon paired signed-rank test by the calculation of the Spearman rank correlation (*r*).

To compare computerized with subjective occlusion rates (OR), we calculated the average OR differences ( $\pm$  SD) of both techniques to histometric OR. Because subjective OR (defined on 3 classes) cannot be correlated with computerized OR/histometric OR (values dispersed for a continuum), no statistical evaluations could be performed for this comparison. GraphPad Instat 3 (GraphPad Software, San Diego, Calif) was used for the statistical procedures.

### Results

The patient-related data and all quantitative angiographic and histometric data are summarized in the Table. Illustrative cases are shown in Figs 1 to 3. Patients had survived embolization

between 2 and 41 days and had died of the initial hemorrhage with refractory vasospasm (*n* = 12), and 1 each had died of cardiorespiratory and renal failure.

Histomorphologic evaluation of the retrieved aneurysms showed, depending on survival times of 2 to 41 days, fresh red static thrombi in the fundus and more fibrin containing white thrombi at the walls (mural thrombi) and in the neck region (Figs 1–3). In the center of the aneurysmal sac, often the coils were located in apparently uncoagulated blood. From 11 days' survival, fibrovascular organization of the more or less coagulated thrombus had started from the aneurysmal walls, with formation of large and perfused sinusoidal vessels around and also within the coils, which were surrounded by multinucleated foreign-body giant cells. After 18 days' survival, the first indication of neointimal formation was observed, starting from the intima of the parent arteries to cover the organized thrombus in the orifice region. Aneurysm #13, after 36 days' survival, demonstrated peripheral fibrovascular organization but delayed organization of a predominately attenuated fibrin clot in the central regions, and a nonoccluded area without neointimal formation on the red and white thrombus in the neck region (Fig 2). However, aneurysm #14, after 41 days'

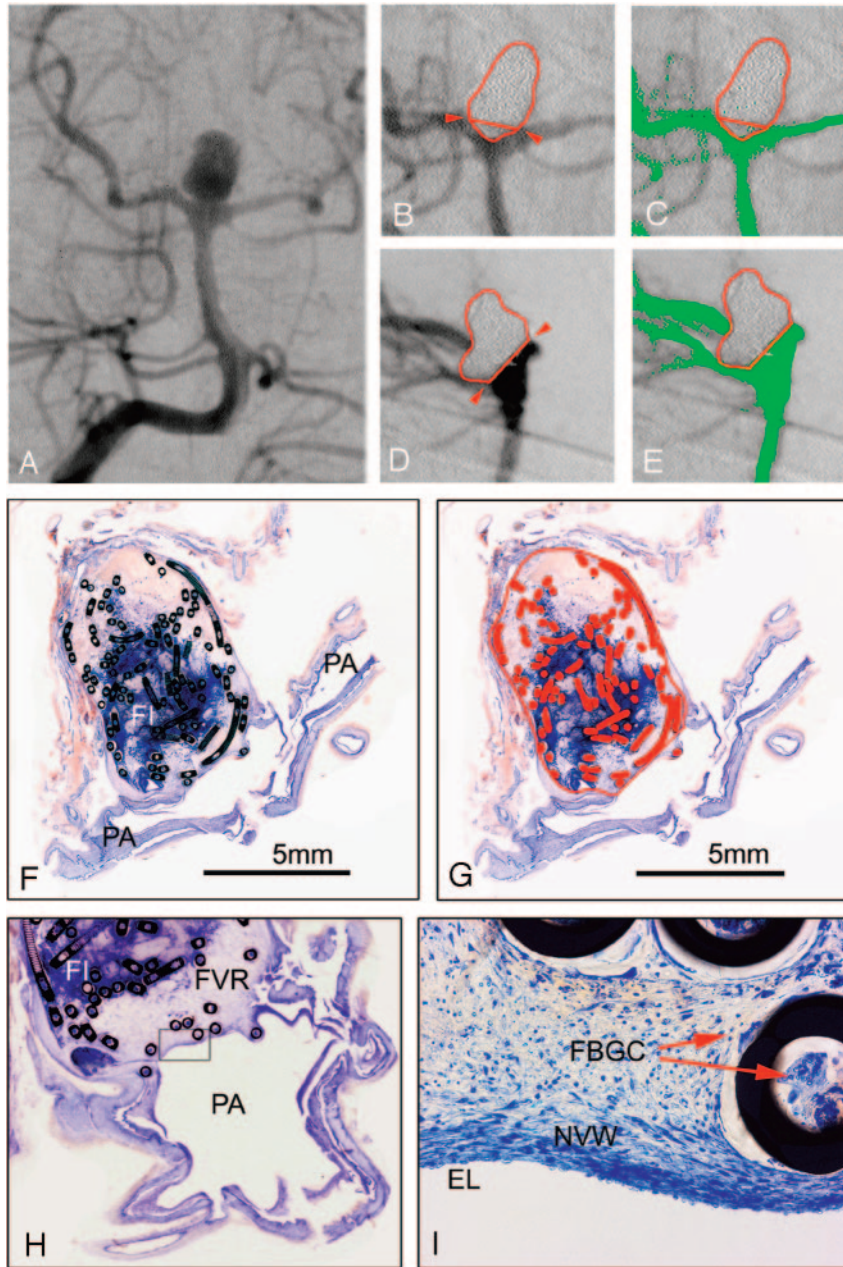


**Fig 3.** A–E, basilar bifurcation aneurysm #14 (female patient; age, 40 years; survival, 41 days) with a subjective and computerized occlusion rate of 100%. A, Preinterventional anteroposterior angiogram. B and C, Enlarged details of the postembolization anteroposterior DSA. C, The aneurysmal border is outlined in red, the neck plane with red arrows. An embolized caudal part of the aneurysm protrudes over the neck plane. D and E, Enlarged details of postembolization lateral DSA projection. D, The protruding part of the aneurysm (B) can be located posteriorly to the basilar artery. On both DSA projections (C and E), no false-color labeled contrast medium inflow into the aneurysm can be discerned. F–I, Micrographs (bar 5 mm) of 2 surface-stained ground sections of aneurysm #14 through the neck region and the parent arteries (PA). F, Note the attenuated blue-stained fibrin clot (FI) in the aneurysmal center. In G, the aneurysmal sac, orifice plane, and metallic coil sections are outlined and labeled in red. No residual inflow area can be discerned and false color labeled in 3 hours. Enlarged detail (magnification 10 ×) from a consecutive ground section, showing a zone of fibrovascular repair (FVR) covering the orifice. I, Further enlarged detail (magnification 140 ×) of the rectangle in 3 hours, showing a new vessel wall (NVW) with endothelial lining (EL). In the organized thrombus, multinucleated foreign-body giant cells (FBGC) can be discerned at the outer and inner coil interfaces (arrows).

survival, showed a similar peripheral thrombus organization and a central fibrin clot but a zone of fibrovascular organization covering the orifice with a new vascular wall, consisting of cells resembling smooth muscle cells, and a neointima with a continuous endothelial lining (Fig 3).

#### Comparison of Angiographic and Histometric Parameters

Statistical evaluation resulted in a nonsignificant difference of computerized angiographic occlusion rate and histometric

OR ( $P = .2163$ ) and a correlation coefficient of  $r = 0.799$  ( $P < .01$ ). Power analysis showed a probability of 99.8% that the difference between the 2 evaluation techniques is lower than 10%, respectively, a probability of 70% for a difference being lower than 5%.

The mean difference between calculated angiographic coil density and measured histometric coil density was 5.8% ( $\pm 3.7$ ), the angiographic values being 1% to 11% higher in 12 cases (Table). In 7 of 14 aneurysms, the differences were 6% or

Comp OR vs. Histo OR (red) Subj OR vs. Histo OR (green)

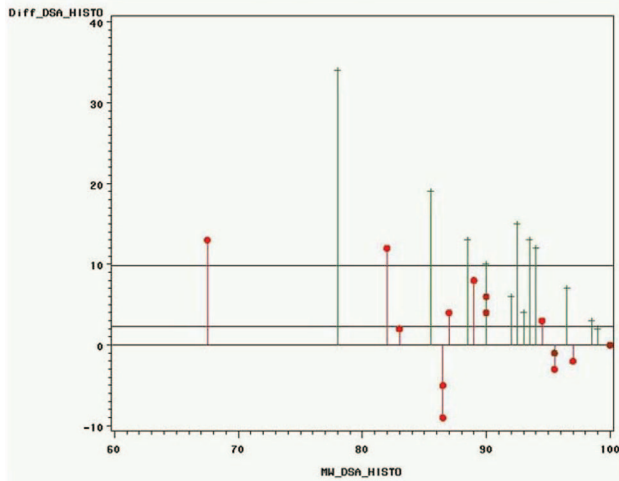


**Fig 4.** Bland-Altman plots comparing the differences of computerized angiographic occlusion rating (*red*) and subjective occlusion rating (*green*) with the reference parameter of the histometric occlusion rate. Especially for the clinically most relevant group of aneurysms with high recanalization, it is shown that the differences are considerably lower for computerized occlusion rating compared with subjective estimations.

greater, with 4 aneurysms having 11% of difference. Statistical comparison resulted in a statistically significant difference ( $P = .0134$ ); the correlation coefficient reached  $r = 0.636$  ( $P < .05$ ).

The mean difference between the measurements of computerized angiographic occlusion rate and histometric occlusion rate was 5.1% ( $\pm 3.8\%$ ). The mean difference between the estimations of subjective angiographic occlusion rate and the measurements of histometric occlusion rate was 10.7% ( $\pm 8.7$ ; Fig 4).

## Discussion

### Comparison of Computerized Angiographic Occlusion Rates with Histometric Occlusion Rates

Before comparing a new diagnostic method to the clinical standard, its correspondence with the real in vivo situation should be evaluated. In our study, this validation was aimed by the comparison of the new computerized angiographic methods with the reference of corresponding histologic ground sections of the aneurysms, displaying the intra-aneurysmal morphologic detail with the highest available resolution power for morphometric quantification.<sup>13-15,22</sup>

The comparison of computerized and histometric occlusion rates in the present series did not result in a statistically significant difference ( $P = .2163$ ) and showed, indeed, a very good correlation ( $r = 0.799$ ;  $P < .001$ ) of computerized angiographic occlusion rating with good statistical power, despite the small sample size of 14 aneurysms.

On the other hand, possible inaccuracy of DSA in displaying the real morphologic features within embolized aneurysms seems indicated by high differences between computerized angiographic and histometric occlusion rates in single cases. In aneurysm #4 with 4 days' survival, a difference of 13% (computerized OR, 74% vs histometric OR, 61%) was measured. For this aneurysm, both methods showed incomplete occlusion of the neck region, but on the serial histologic

ground sections, the nonoccluded area was considerably larger. One possible explanation for these high differences of occlusion rates may be that considerable changes of aneurysmal occlusion rates and, thus, aneurysmal stability occurred already in the first days after embolization.

### Comparison of Angiographic and Histometric Coil Densities

The comparison of angiographic and histometric coil densities resulted in a statistically significant difference of the 2 evaluation techniques. Despite acceptable correlation ( $r = 0.636$ ;  $P < .05$ ), these findings of significant statistical difference may not justify wide clinical application angiographic coil density calculations. As in a total of 4 aneurysms, differences of 11% were unacceptably high (Table).

The main reason for these high differences was the complex anatomy of the respective aneurysms. Because of this complex aneurysmal shape, the approximation of the aneurysmal volume as ellipsoid volume was inaccurate for these cases. Thus, we believe that the limitation of indirect approximation of the aneurysm as ellipsoid volume has to be overcome before clinical introduction of this method. The solution for this problem would be direct aneurysmal volume measurements performed on 3D DSAs or MR angiographies (MRAs). With this possibility of direct volumetry coil density, calculations may reach clinically acceptable correspondence also for aneurysms with complex aneurysmal morphologic features.

### Comparison of Computerized Angiographic Occlusion Rates with Subjective Angiographic Occlusion Rates

To evaluate a possible benefit of new methods, these must be compared with the standard clinical procedure. In experimental aneurysms, the theoretic benefits of computerized angiographic occlusion rating have already been shown.<sup>14</sup>

Comparable with the findings of the above-cited experimental study, also in the present human aneurysmal series, 12 of 14 aneurysms showed lower computerized OR values compared with subjective angiographic estimations. Besides several methodologic factors listed in the limitation section below, a major reason for this tendency to lower computerized angiographic OR values seems to be the higher-resolution power of the computerized gray value definition of the contrast medium in the parent arteries. Subjective OR estimation is apparently not that precise in recognition of all intra-aneurysmal contrast medium gray values in DSA. Thus, smaller contrast medium-filled intra-aneurysmal areas are subjectively underestimated, leading to higher subjective OR values. Another reason may be the better aneurysmal border definition with computerized methods. For example, in aneurysm #4, this factor led to OR differences of 21% (subjective OR, 95% vs computerized OR, 74%). The computerized method could provide better aneurysmal border definition with the possibility of image superimposition of the corresponding pre-embolization and postembolization images.

All these above-mentioned factors resulted in a relatively high mean difference of 10.7% ( $\pm 8.7$ ) between subjective OR and histometric OR compared with a substantial lower mean difference of just 5.1% ( $\pm 3.8$ ) between computerized OR and histometric OR. Especially for the clinically most relevant group of aneurysms with high recanalization, the new com-

puterized techniques showed substantially lower differences (Fig 4): For the aneurysms with the highest histometric recanalization (aneurysm #2: histometric OR, 76%; aneurysm #4: histometric OR, 61%), the differences to computerized OR were 12% (aneurysm #2) and 13% (aneurysm #4) compared with considerably higher differences of 19% (aneurysm #2) and 34% (aneurysm #4) for subjective OR estimations.

Therefore, compared with subjective OR estimations, computerized OR (despite the remaining high differences) provided a clinically relevant benefit for aneurysms with high recanalization. This finding avoids possible subjective OR overestimations that theoretically would result in delayed re-embolization. These findings may be an important contribution to future necessary subclassifications of Roy class 2 and 3 aneurysms. With computerized angiographic occlusion rating, the definition of more objective angiographic occlusion-rate cutoff values for evidence-based re-embolization indications could be theoretically possible for the first time.

For Roy class 1 aneurysms, and also for nearly completely occluded Roy class 2 aneurysms (99% or 98% computerized OR), subjective OR estimations are equivalent to computerized OR. This seems intuitive, as it is, of course, easier to subjectively define complete filling than to precisely estimate a certain degree of recanalization. In addition, for these aneurysms, additional subclassifications are clinically not relevant because these aneurysms are known to remain stable.

It should be mentioned that computerized occlusion rating requires nearly no additional clinical effort in our experience. Finally, it should be emphasized that the new technique of computerized angiographic occlusion rating is preliminary. Of course, this tool has to prove its clinical value in larger angiographic application trials before transfer to clinical practice.

### **Limitations of the Present Findings**

The theoretic analytic limitations of the present findings are the following:

1. The 2 different time points of angiographic evaluation and postmortem histometry could lead to different results because of the dynamic processes of scar formation and recanalization. Because angiography and, thus, computerized occlusion rating cannot distinguish between the absence of flow from thrombus formation vs the absence of flow from coils, it is a limitation to the present findings to compare the 2 techniques, when the time points vary much. We tried to minimize this factor by the selection of “early” postembolization aneurysms.
2. The comparison of histologic ground sections with DSA images, representing the whole aneurysmal volume, with coils in front or behind, possibly hiding empty recanalized aneurysm areas was another theoretic limitation. We tried to minimize this limitation by selecting DSA projections, providing a representative overview of the aneurysmal occlusion focusing on the recanalized neck together with the length axis of the aneurysms and, in cases of complex aneurysmal anatomy, with the careful selection of a second representative projection plane. Comparable with the estimations of subjective occlusion rating, a careful DSA selection remains the main factor for valid measurements of

computerized occlusion rating. To guarantee clinical applicability without extensive time-consuming procedures, we limited the evaluations to 2 DSA projections in our study, which was another limitation to the present findings.

3. Theoretically shrinking artifacts from specimen preparation and embedding techniques of the histologic ground sections could lead to inaccurate histometric measurements. It could be shown that the problem of shrinking artifacts and collapse of the histologic ground sections theoretically leading to evaluation bias can be avoided with correct perfusion fixation and with polymethylmethacrylate embedding with the coils in situ functioning like a frame for the soft tissue.<sup>13-15,22</sup> These data proved the favorable comparability of histologic ground sections with angiographic images. Furthermore, aneurysms nevertheless showing shrinking artifacts were excluded from this study, as mentioned in the Methods section.
4. The morphometry of 2D images for 3D structures was another limitation. With the above-described careful selection of the respective DSA projections, together with corresponding histologic ground section planes, we tried to minimize this limitation. This limitation was demonstrated especially by aneurysm #13 (Fig 2). This emphasizes the need of 3D DSA or even noninvasive 3D MRA for future quantitative evaluations. Direct 3D aneurysmal volumetry also seems crucial for the clinical application of coil density calculations.
5. A limitation for statistical findings may have been the small sample size that was nevertheless equivalently respectively higher as in nearly all published human histopathologic studies.<sup>7-13,23-26</sup>
6. The subjective OR estimations had been performed by the same physician, who then did the selection of the DSA projections and the definitions of the angiographic parameters for additional evaluations.

We are well aware of all these methodologic shortcomings. However, the present clinical standard of subjective occlusion rating is limited also by nearly all of the above-cited shortcomings. Therefore, there remain the benefits of the objective computerized occlusion rating. Contrary to computerized OR, the present clinical standard of subjective OR estimations cannot provide a subclassification of the clinically most relevant group of “residual aneurysms” and, thus, limits any evidence-based cutoff value definition for aneurysmal re-embolization.

### **Conclusions**

1. Computerized angiographic occlusion rating showed better correspondence with histometry compared with subjective angiographic occlusion rating, especially for the clinically most relevant group of aneurysms with high recanalization. Better definition of aneurysmal borders and contrast medium inflow was superior to the present clinical standard of subjective OR estimations. Thus, clinical application of computerized occlusion rating seems theoretically feasible. For recanalized aneurysms, this tool may be important for the definition of evidence-based cutoff val-



ues for re-embolization, especially with the use of 3D volumetry of DSA or MRA.

2. Coil density calculations are limited in their clinical value by the approximation of the aneurysm as ellipsoid volume. This limitation probably can be overcome by direct aneurysmal volumetry with use of 3D DSA or MRA.

## References

1. Molyneux A, Kerr R, Stratton I, et al. **International Subarachnoid Aneurysm Trial (ISAT) Collaborative Group. International Subarachnoid Aneurysm Trial (ISAT) of neurosurgical clipping versus endovascular coiling in 2143 patients with ruptured intracranial aneurysms: a randomised trial.** *Lancet* 2002;360:1267–74
2. Molyneux A, Kerr R, Yu LM, et al. **International Subarachnoid Aneurysm Trial (ISAT) Collaborative Group. International Subarachnoid Aneurysm Trial (ISAT) of neurosurgical clipping versus endovascular coiling in 2143 patients with ruptured intracranial aneurysms: a randomized comparison of effects on survival, dependency, seizures, rebleeding, subgroups, and aneurysm occlusion.** *Lancet* 2005;366:809–17
3. Guglielmi G, Vinuela F, Sepetka I, et al. **Electrothrombosis of saccular aneurysms via endovascular approach.** *JNS J Neurosurg* 1991;75:1–7
4. Bryan RN, Rigamonte D, Mathis JM. **The treatment of acutely ruptured aneurysms: endovascular therapy versus surgery.** *AJNR Am J Neuroradiol* 1997;18:1826–30
5. Cloft H, Kallmes D. **Aneurysm packing with HydroCoil embolic system versus platinum coils: initial clinical experience.** *AJNR Am J Neuroradiol* 2004;25:60–62
6. Taschner C, Leclerc X, Rachdi H, et al. **Matrix detachable coils for the endovascular treatment of intracranial aneurysms: analysis of early angiographic and clinical outcomes.** *Stroke* 2005;36:2176–80
7. Szikora I, Seifert P, Hanzely Z, et al. **Histopathologic evaluation of aneurysms treated with Guglielmi detachable coils or Matrix detachable microcoils.** *AJNR Am J Neuroradiol* 2006;27:283–88
8. Raymond J, Guilbert F, Metcalfe A, et al. **Role of endothelial lining in recurrences after coil embolization.** *Stroke* 2004;35:1471–75
9. Barrocas A, Derdeyn C, Cross D 3rd, et al. **Histologic and hemodynamic effects of endosaccular platinum coils for intracranial aneurysms.** *J Long Term Eff Med Implants* 2004;14:225–42
10. Groden C, Hagel C, Delling G, et al. **Histological findings in ruptured aneurysms treated with GDCs: six examples at varying times after treatment.** *AJNR Am J Neuroradiol* 2003;24:579–84
11. Mori K, Nakao Y, Horinaka N, et al. **Cerebral aneurysm regrowth and coil unravelling after incomplete Guglielmi detachable coil embolization: serial angiographical and histological findings.** *Neurol Med Chir (Tokyo)* 2003;43:293–97
12. Asai J, Suzuki R, Fujimoto T, et al. **Correlation of magnetic resonance imaging and histological findings in a large basilar tip aneurysm after coil embolization: case report.** *Neurol Med Chir (Tokyo)* 2000;40:519–23
13. Bavinszki G, Talazoglu V, Killer M, et al. **Gross and microscopic histopathological findings in aneurysms of the human brain treated with Guglielmi detachable coils.** *JNS J Neurosurg* 1999;91:284–93
14. Sherif C, Plenk H Jr, Grossschmidt K, et al. **Computer-assisted quantification of occlusion and coil densities on angiographic and histological images of experimental aneurysms.** *Neurosurgery* 2006;58:559–66
15. Cruise GM, Shum JC, Plenk H Jr. **Hydrogel-coated and platinum coils for intracranial aneurysm embolization compared in three experimental models using computerized angiographic and histologic morphometry.** *J Mater Chem* 2007;17:3965–73
16. Tamatani S, Ito Y, Abe H, et al. **Evaluation of the stability of aneurysms after embolization using detachable coils: correlation between stability of aneurysms and embolized volume of aneurysms.** *AJNR Am J Neuroradiol* 2002;23:762–67
17. Yoshino Y, Niimi Y, Song J, et al. **Endovascular treatment of intracranial aneurysms: comparative evaluation in a terminal bifurcation aneurysm model in dogs.** *JNS J Neurosurg* 2004;101:996–1003
18. Sluzewski M, van Rooij W, Slob MJ, et al. **Relation between aneurysm volume, packing, and compaction in 145 cerebral aneurysms treated with coils.** *Radiology* 2004;231:653–58
19. Yagi K, Satoh K, Satomi J, et al. **Evaluation of aneurysm stability after endovascular embolization with Guglielmi detachable coils: correlation between long-term stability and volume embolization ratio.** *Neurol Med Chir (Tokyo)* 2005;45:561–66
20. Kawanabe Y, Sadato A, Taki W, et al. **Endovascular occlusion of intracranial aneurysms with Guglielmi detachable coils: correlation between coil packing density and coil compaction.** *Acta Neurochir* 2001;143:451–55
21. Roy D, Milot G, Raymond J. **Endovascular treatment of unruptured aneurysms.** *Stroke* 2001;32:1998–2004
22. Plenk H Jr. **The microscopic evaluation of hard tissue implants.** In Williams DF, ed. *Techniques of Biocompatibility Testing*. Vol 1. Boca Raton, Florida: CRC Press; 1986:35–81
23. Castro E, Fortea F, Villoria F, et al. **Long-term histopathological findings in two cerebral aneurysms embolized with Guglielmi detachable coils.** *AJNR Am J Neuroradiol* 1999;20:549–52
24. Strother C, Berenstein A, Vinuela F. **A pitfall in the surgery of a recurrent aneurysm after coil embolization and its histological observation: technical case report.** *Neurosurgery* 1998;42:1199–200
25. Stiver S, Porter P, Willinsky R, et al. **Acute human histopathology of an intracranial aneurysm treated using Guglielmi detachable coils: case report and review of literature.** *Neurosurgery* 1998;43:1203–08
26. Molyneux A, Ellison D, Morris J, et al. **Histological findings in giant aneurysms treated with Guglielmi detachable coils: report of two cases with autopsy relation.** *JNS J Neurosurg* 1995;83:129–32